

# Superresolution Reconstruction of Infra-red Image Sequences by Wavelet Expansion

Jun Li

COPL, Physics department  
Laval University  
Ste-Foy, Quebec, G1K 7P4, Canada  
[jLi@phy.ulaval.ca](mailto:jLi@phy.ulaval.ca)

Yunlong Sheng

COPL, Physics department  
Laval University  
Ste-Foy, Quebec, G1K 7P4, Canada  
[Sheng@phy.ulaval.ca](mailto:Sheng@phy.ulaval.ca)

Léandre Sévigny

Defence Research Establishment Valcartier,  
2459 Boul. Pie XI nord, Val-Belair,  
Quebec, G3J 1X5, Canada  
[Leandre.sevigny@drev.dnd.ca](mailto:Leandre.sevigny@drev.dnd.ca)

Pierre Valin

Lockheed Martin Electronic Systems Canada,  
6111 Royalmount Ave., Montreal,  
Quebec, H4P 1K6, Canada  
[Pierre.valin@lmco.ca](mailto:Pierre.valin@lmco.ca)

## Abstract

Many automatic target recognition, detection, and identification problems usually suffer from lack of adequate resolution of the image data. The undersampling is a common problem among infrared imaging systems. One often desires to obtain a higher resolution image from multiframe of undersampled low-resolution images. In this paper, a new superresolution reconstruction algorithm combining Bayesian Maximum a Posteriori estimator and wavelet transformation is proposed for infrared (IR) aerial image sequences. The multiframe wavelet expansions are placed into a Bayesian framework to form a MAP estimate of the high-resolution scene from a sequence of undersampled low-resolution frames. In this approach, both of the image sequences and the degradation operator to be inverted are represented by wavelet expansions. Minimizing the regularization cost function based on wavelet expansion forms the high-resolution estimate. This provides a unified approach for deblurring, noise removal, and high resolution reconstruction from a low-resolution, blurred, and noisy infrared image sequence. This method has been tested and verified on the infrared aerial image sequence DIM01 provided by Defence Research Establishment Valcartier. Compared with the IBP and gradient descent approaches, the proposed scheme is more effective for noise removal than the IBP ones. The number of iterations by the proposed approach is less than that by the gradient descent approach.

## Index Terms

Superresolution, Wavelet expansion, Minimization, MAP, IR image sequences.

## 1. Introduction

Images are recorded to portray useful information about a phenomenon of interest. Unfortunately, a recorded image will almost certainly be a degraded version of an original image or scene due to the imaging optics, sensor noise, and sampling of the continuous scene on an arbitrary space-time lattice. A number of restoration algorithms for a single image were proposed in the last three decades [1]-[3]. Recent studies are mostly focused on the so-called second-generation restoration problems, which are multiple image restoration [4]-[6] and superresolution image restoration [7]-[21].

Superresolution refers to methods for increasing the resolving power by recapturing additional high-frequency information from adjacent frames in a sequence that contains slightly different, but unique, information. The superresolution restoration was first introduced by Tsai and Huang [7]. Their motivation was for generating a high-resolution frame from misregistered Landsat images. They used a frequency domain approach to reconstruct one improved resolution image from several undersampled noise-free images. An extension of this algorithm for noisy data was provided by Kim et al [8]. Irani and Peleg [9] proposed the iterative backprojection (IBP) method for the superresolution restoration. They estimated an initial guess for the high-resolution image, and simulated the imaging process to obtain the temporary result to the measurements. Then they updated the temporary guess according to this simulation error. The superresolution algorithm for the restoration of high-resolution image from several geometrically warped, blurred, noisy and undersampled measured images was suggested by Elad and Feuer [11]. Srinivas and Srinath [12] proposed a multiple image

superresolution restoration algorithm based on a minimum squared error (MMSE) approach and on the interpolation of the restored images into a single image. Cain et al. [13] developed a maximum likelihood (ML) technique using an expectation maximization algorithm for the high-resolution image reconstruction. Hardie et al. [14]-[16] extended the IBP method. They employed a gradient descent and a conjugated-gradient technique for minimizing the cost function that is the total squared error between the observed low-resolution data and the predicted low-resolution data. Set theoretic approach to this problem was also suggested by Stark and Oskoui [17]. They formulated a projection onto convex sets (POCS) algorithm to estimate a superresolution image from observations, which are obtained by scanning or rotating an image with respect to the CCD image acquisition sensor array. Tekalp et al. [18] then extended this POCS formulation to include sensor noise. Patti joined with Tekalp to account for time-varying motion blur within video sequences, and to accommodate for interlaced frames and other video sampling patterns [19]. Elad and Feuer [11] utilized the existing superresolution algorithms such as ML, MAP and POCS to propose a unified methodology toward the more complicated problem of superresolution restoration. This approach is general but assumes explicit knowledge of linear space- and time-variant blurs, additive Gaussian noise, different measured resolution, and motion characteristics.

Superresolution image restoration methods clearly are better adapted for processing infrared image sequences. However, existing methods suffer from two shortcomings: 1). It is particular important for the superresolution image restoration problem to process noise, since wide-band noise mainly affects high-frequency information to be recaptured. All existing methods resort to some sort of iterative regularization to overcome the problem. The challenge is how to regularize so that the high-frequency data are not smoothed out. 2). Most existing methods are slow to converge because the variables of observed images are not sufficiently "de-correlated" or diagonalized. The better solution to this problem could be an orthogonal decomposition of the image.

In order to overcome the shortcomings of the existing methods, we propose, in this paper, a new superresolution reconstruction approach based on combining Bayesian Maximum a Posteriori estimator with wavelet transformation and apply it to superresolution image reconstruction of infra-red (IR) sequences. The wavelet expansion method for solution of inverse problem of a single image from linear blur and additive noise was introduced by Wang et al. [22]. This method expanded both degradation operator and observed image by wavelets and solved for the wavelet coefficients of original image. It has been demonstrated that wavelet expansions not only achieved data decorrelation and multi-grid processing, they

also provided a general and consistent scheme for representing the inverse problem at multiple resolutions. Furthermore, wavelets provide efficient or "sparse" representations for both the operator and the image. In our approach, the multiframe wavelet expansions are placed into a Bayesian framework to form a MAP estimate of the high-resolution scene from a sequence of undersampled low-resolution frames. The paper is organized as follows. The observation model is described in section 2. Section 3 presents a new model for the superresolution problem based on combining wavelet-based approach with MAP estimator. Experimental results are presented in section 4.

## 2. Observation Model

In this section we start with an intimate understanding of the degradation processes that operate on the scene information during the acquisition of image sequences of undersampled low-resolution frames, and then to introduce an analytical model describing it.

A block diagram of the discrete observation model is shown in Fig.1. Assume that we observe  $N$  frames,  $v_k(x, y)$  for  $k = 1, 2, \dots, N$ . Each observed frame in a low-resolution image sequences contains  $M_1 \times M_2$  square pixels. These data in lexicographical notation will be expressed as a vector  $\mathbf{v}_k = [v_{k,1}, v_{k,2}, \dots, v_{k,M}]^T$ , where  $M = M_1 \times M_2$ . Let  $u(x, y)$  represent the ideal or desired high-resolution image, which is of dimensions  $P = LM_1 \times LM_2$ . This image is assumed to be sampled at the Nyquist rate, and is not blurred by the imaging system in any way. Here  $L$  is the downsampling factor in the model. In a lexicographical format, the idea image is written as

$$\mathbf{u} = [u_1, u_2, \dots, u_P]^T \quad (1)$$

The observation model between the desired image  $\mathbf{u}$  and the observed frames  $\mathbf{v}$  can be expressed in simple form where the low-resolution pixels are defined as weighted sums of appropriate high-resolution pixels with additive noise [14]. This generalized form can allow for point spread function (PSF) blurring, geometric transformation, and subsampling of the high-resolution images. Thus, the observed low-resolution pixels from frame  $k$  are related to the high-resolution images as follows:

$$v_{k,m} = \sum_{r=1}^P w_{k,m,r} \cdot u_r + \eta_{k,m} \quad (2)$$

For  $m = 1, 2, \dots, M$  and  $k = 1, 2, \dots, N$ . The weight  $w_{k,m,r}$  represents the contribution of the  $r$ th high-resolution pixel in  $\mathbf{u}$  to the  $m$ 'th low-resolution pixel in the  $k$ th frame  $\mathbf{v}_k$ . These weights depend on the position of each pixel with respect to the fixed grid defined by  $\mathbf{u}$  and the system PSF.

For the observed frames by registering all the low-resolution images over a fixed finer grid, the observation model for the  $k$ 'th frame can be expressed in matrix notation as

$$\mathbf{v}_k = \mathbf{T}_k \cdot \mathbf{u} + \boldsymbol{\eta}_k \quad (3)$$

Where  $\mathbf{T}_k$  is a degradation matrix,  $\mathbf{v}_k$  is the  $k$ th observed

spatially adaptive operation that enforces smoothness constraints for the regularization. The estimation errors in the high-frequency and the low-frequency bands is performed separately, resulting in fast-convergence.

Given the observed values, the MAP estimate is performed by maximizing the conditional probability density function of the ideal image  $P(\mathbf{u} | \mathbf{v})$ . Based on the Bayes rule, maximizing  $P(\mathbf{u} | \mathbf{v})$  is equivalent to maximizing the function  $P(\mathbf{v} | \mathbf{u})P(\mathbf{u})$  [1]-[2]. If we assume that observed additive noise is zero mean Gaussian random process and  $\mathbf{u}$  is a zero mean Gaussian random process, we can use the ML estimator for the MAP estimator. Thus, the high-resolution image reconstruction is performed by the minimization of a cost function. The cost function is derived from the observation model Eq. (3). Here, the minimization of the cost function can be

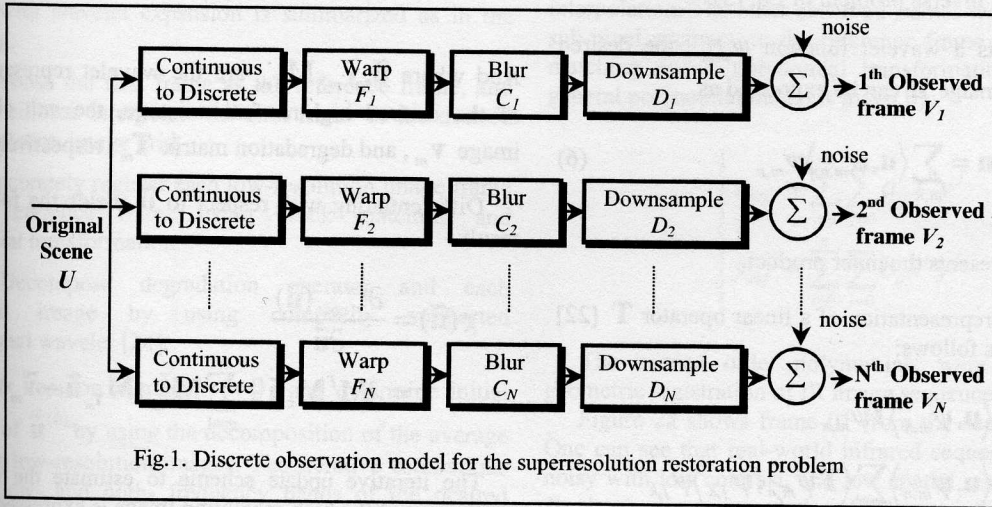


Fig.1. Discrete observation model for the superresolution restoration problem

image,  $\mathbf{u}$  represents the desired high-resolution image, defined as and  $\boldsymbol{\eta}_k$  stands for the additive noise in the  $k$ th frame.

$$\hat{\mathbf{u}} = \arg \min_{\mathbf{u}} C_{\text{cost}}(\mathbf{u}) \quad (4)$$

Where the cost function is written as

$$C_{\text{cost}}(\mathbf{u}) = \frac{1}{2} \sum_{m=1}^N \|\mathbf{T}_m \mathbf{u} - \mathbf{v}_m\|^2 + \frac{\lambda}{2} \|\mathbf{C} \cdot \mathbf{u}\|^2 \quad (5)$$

### 3. Bayesian Superresolution Reconstruction by wavelet expansion

One wants to estimate from Eq. (3) the desired high-resolution image  $\mathbf{u}$  from all observed images  $\mathbf{v}_k$  ( $k = 1, 2, \dots, N$ ). It is an ill-posed problem. In order to overcome the shortcomings of the existing methods, a wavelet-based approach to superresolution restoration from multi-frame image sequences is presented in this section. Wavelet expansions not only implement data decorrelation, but also provide efficient or "sparse" representations for both the operator and the image, and allow a simple

And where  $\|\cdot\|$  is the  $L^2(R)$  norm,  $\mathbf{C}$  is a regularizing operator,  $\lambda$  is a positive regularizing parameter and  $\hat{\mathbf{u}}$  is the high-resolution image estimate. It can be shown that Eqs. (4) and (5) is a maximum a posteriori estimate in the case of Gaussian noise.

The first term in Eq. (5) is the sum of squared differences between the observed low-resolution image vectors  $\mathbf{v}_m$  and the low-resolution estimation vectors that are predicted by the observation Eq. (3). However, direct minimization of this term alone can lead to a poor estimate due to the ill-posed nature of the inverse problem, whose solution is not unique. The second term in Eq. (5) is a penalty or a constraint term that regularizes the inverse problem. A popular choice for the regularizing operator  $\mathbf{C}$  is the second-derivative operator that corresponds to a smoothing constraint. The second term will tend to minimum when the image estimate  $\mathbf{u}$  is smooth. The parameter  $\lambda$  in the regularization term controls the trade-off between two types of errors in cost function. A large value for  $\lambda$  will tend to yield a smooth solution, while a low value for  $\lambda$  will lead to the noise magnification.

Next we will discuss how to describe the wavelet representation of inverse problem of Eq. (3).

If there exists a wavelet function  $\psi_{m,n}$ , the desired high-resolution image  $\mathbf{u}$  can be expressed as

$$\mathbf{u} = \sum_{m,n} \langle \mathbf{u}, \psi_{m,n} \rangle \psi_{m,n} \quad (6)$$

Where  $\langle \cdot, \cdot \rangle$  represents the inner product.

The wavelet representation of a linear operator  $\mathbf{T}$  [22] can be derived as follows:

$$\begin{aligned} \mathbf{T}\mathbf{u} &= \sum_{m,n} \langle \mathbf{u}, \psi_{m,n} \rangle \mathbf{T}\psi_{m,n} \\ &= \sum_{m,n} \langle \mathbf{u}, \psi_{m,n} \rangle \sum_{j,k} \langle \mathbf{T}\psi_{m,n}, \psi_{j,k} \rangle \psi_{j,k} \\ &= \sum_{j,k} \left[ \sum_{m,n} \langle \mathbf{u}, \psi_{m,n} \rangle \langle \mathbf{T}\psi_{m,n}, \psi_{j,k} \rangle \right] \psi_{j,k} \end{aligned} \quad (7)$$

In the above expansion, the operator  $\mathbf{T}$  is completely determined by the wavelet expansion coefficients of  $\mathbf{T}\psi_{m,n}$ . Thus, the wavelet expansion of the operator  $\mathbf{T}$  can be obtained by the same way as that of a signal. Furthermore, if compactly supported wavelets are used, there will be only a finite number of nonzero coefficients.

Let  $\mathbf{M}_T$  be a matrix representation of  $\mathbf{T}$  by wavelet expansion. The original function equation (3) can be now represented as a matrix equation of wavelet expansion coefficients:

$$\tilde{\mathbf{v}}_k = \mathbf{M}_{T_k} \tilde{\mathbf{u}} + \tilde{\mathbf{w}}_k \quad (8)$$

Where  $\tilde{\mathbf{v}}_k, \tilde{\mathbf{u}}, \tilde{\mathbf{w}}_k$  are vectors whose components are wavelet expansion coefficients of  $\mathbf{v}_k, \mathbf{u}$ , and  $\boldsymbol{\eta}_k$ , respectively.

Equation (8) shows that the solution of inverse problem for a signal or an image can be converted into that for a set of wavelet expansion coefficients.

Assuming that  $\mathbf{M}_c$  is the wavelet representation of the linear operator  $\mathbf{C}$ , the regularized solution based on wavelet representation can be expressed as

$$\hat{\tilde{\mathbf{u}}} = \arg \min_{\tilde{\mathbf{u}}} C_{\text{cost}}(\tilde{\mathbf{u}}) \quad (9)$$

Where the cost function is written as

$$C_{\text{cost}}(\tilde{\mathbf{u}}) = \frac{\lambda}{2} \|\mathbf{M}_c \cdot \tilde{\mathbf{u}}\|^2 + \frac{1}{2} \sum_{m=1}^N \|\mathbf{M}_{T_m} \tilde{\mathbf{u}} - \tilde{\mathbf{v}}_m\|^2 \quad (10)$$

And where  $\tilde{\mathbf{u}}, \tilde{\mathbf{v}}_m, \mathbf{M}_{T_m}$  are the wavelet representations of the desired high-resolution image, the  $m$ th observed image  $\mathbf{v}_m$ , and degradation matrix  $\mathbf{T}_m$ , respectively.

Differentiating with respect to  $\tilde{\mathbf{u}}$  yields the following result:

$$\begin{aligned} g(\tilde{\mathbf{u}}) &= \frac{\partial C_{\text{cost}}(\tilde{\mathbf{u}})}{\partial \tilde{\mathbf{u}}} \\ &= \lambda \mathbf{M}_c^T \mathbf{M}_c \tilde{\mathbf{u}} + \sum_{m=1}^N \mathbf{M}_{T_m}^T (\mathbf{M}_{T_m} \tilde{\mathbf{u}} - \tilde{\mathbf{v}}_m) \end{aligned} \quad (11)$$

The iterative update scheme to estimate the wavelet coefficient of the high-resolution image is expressed by

$$\hat{\tilde{\mathbf{u}}}^{n+1} = \hat{\tilde{\mathbf{u}}}^n - \varepsilon^n g(\tilde{\mathbf{u}}^n) \quad (12)$$

Where, the parameter  $\varepsilon^n$  is the step size at the  $n$ th iteration. The optimal step size can be calculated by minimizing the updated cost function

$$C_{\text{cost}}(\hat{\tilde{\mathbf{u}}}^{n+1}) = C_{\text{cost}}(\hat{\tilde{\mathbf{u}}}^n - \varepsilon^n \mathbf{g}^n) \quad (13)$$

Where

$$\mathbf{g}^n = \begin{bmatrix} g(\hat{u}_1^n) \\ g(\hat{u}_2^n) \\ \vdots \\ g(\hat{u}_p^n) \end{bmatrix} \quad (14)$$

With respect to  $\mathcal{E}^n$ , that gives the following result:

$$\mathcal{E}^n = \frac{(\mathbf{g}^n)^T \sum_{m=1}^N \mathbf{M}_{T_m}^T (\sum_{m=1}^N \mathbf{M}_{T_m} \hat{\mathbf{u}}^n - \mathbf{v}_m) + \lambda (\mathbf{g}^n)^T \mathbf{M}_c^T \mathbf{M}_c \hat{\mathbf{u}}^n}{(\mathbf{g}^n)^T (\sum_{m=1}^N \mathbf{M}_{T_m}^T \mathbf{M}_{T_m}) \mathbf{g}^n + \lambda (\mathbf{g}^n)^T \mathbf{M}_c^T \mathbf{M}_c \mathbf{g}^n} \quad (15)$$

The iteration with Eq. (12) continues until the cost function stabilizes or falls below a predetermined threshold  $\tau$ , such that

$$\frac{\|\hat{\mathbf{u}}^{n+1} - \hat{\mathbf{u}}^n\|}{\|\hat{\mathbf{u}}^n\|} \leq \tau \quad (16)$$

The final estimate is given as  $\hat{\mathbf{u}} = \hat{\mathbf{u}}^{n+1}$ . The iterative process with wavelet expansion is summarized as in the following.

1). Choose the first frame as the reference frame, and spatially bilinear interpolate the first frame to the desired high-resolution image grid.

2). Accurately register each low-resolution image frame to the reference frame using block matching and polynomial transformation.

3). Decompose degradation operator and each registered image by using compactly supported orthonormal wavelet [24].

4). Set iteration number  $n = 0$ , and determine initial estimate of  $\hat{\mathbf{u}}^{(0)}$  by using the decomposition of the average of all the low-resolution images. The iterative estimations of both low- and high- frequency bands of the desired high-resolution image are performed independently in the same steps as follows:

a). Compute the residual  $g(\hat{\mathbf{u}}^n)$  according to Eq. (11).

b). Update the estimate:  $\hat{\mathbf{u}}^{n+1} = \hat{\mathbf{u}}^n - \mathcal{E}^n g(\hat{\mathbf{u}}^n)$ .

Where the optimal step size  $\mathcal{E}^n$  is computed using Eq. (15)

c). If the criterion (16) is satisfied, then  $\hat{\mathbf{u}} = \hat{\mathbf{u}}^{n+1}$ . Otherwise, increment  $n$  and return to step 4).

5). Implement inverse wavelet transformation to obtain the reconstructed image.

#### 4. Experimental Results

In order to demonstrate the effectiveness of the proposed approach for superresolution reconstruction, a sequence

(DIM) of IR images 20 frames was used in the experiments. The sequence was acquired at a 4 Hz frame rate by a helicopter mounted infrared camera. The 20 images were downsampled to  $(184 \times 108)$  size, were used as the input frames. We want to reconstruct a single high-resolution image of  $(368 \times 216)$  size.

For convenience, define the first observed frame to be the reference frame, and without loss of generality, let the reference image be of the same size as the desired high-resolution image by conventional up-sampling and bilinear interpolation. The other observed frames were registered at sub-pixel accuracy to the reference frame by using block matching and a polynomial transformation model. The general polynomial model is given by:

$$\begin{cases} x_{ref} = \sum_{i=0}^n \sum_{j=0}^n a_{ij} x^i y^j \\ y_{ref} = \sum_{i=0}^n \sum_{j=0}^n b_{ij} x^i y^j \end{cases} \quad (16)$$

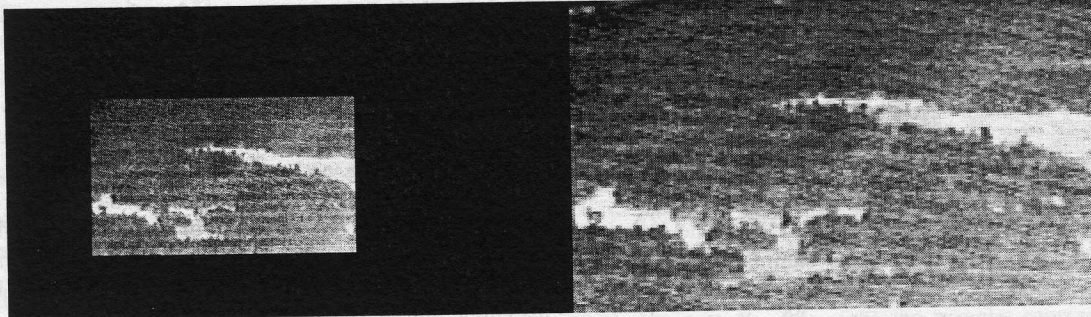
The second order polynomials were used for the geometric registration of IR image sequences here.

Figure 2a shows frame 01 from the sequence DIM01. One can see that real-world infrared sequence images are noisy with low contrast, and low spatial resolution. Figure 2b shows the up-sampled and bilinear interpolated frame 01. Actually, interpolating by using Shannon's expansion is equivalent to decomposing the frame on the standard orthonormal basis, and then ideal low-pass filtering for reconstruction on a denser basis. It is apparent that lower-order interpolation such as bilinear would yield lower-quality images. Figure 2c is the average of all the 20 registered low-resolution frames. The noises are clearly diminished in this image, but the image exhibits a visually unsatisfactory blur, and the block artifact still occurs in the average image. Applying the proposed superresolution reconstruction algorithm yielded the image shown in Figure 2d. In the experiment, the regularization parameter with  $\lambda = 0.05$  was used. A standard Laplacian operator is used for the regularizing operator  $\mathbf{C}$ . Here we use a two-dimensional Gaussian function for the sensor PSF. The spread parameter of the Gaussian function was taken to be equal to the blur parameter, and therefore the PSF was:

$$PSF(x, y) = \frac{1}{2\pi\sigma^2} \exp\left(-\frac{x^2 + y^2}{2\sigma^2}\right) \quad (17)$$

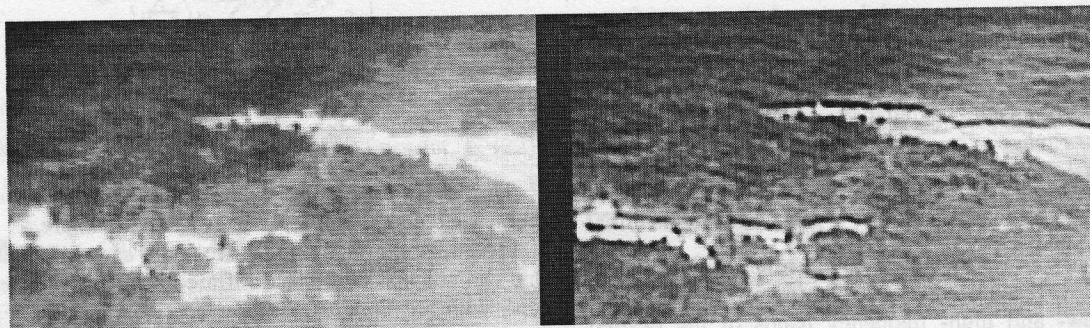
Thus, the degradation operator can be obtained from the sensor PSF. A total of four iterations of the reconstruction algorithm were performed. One can see the clear recovery of the edges in the island in the

superresolved image as compared with the artifacted version obtained by interpolation of Fig. 2b. Therefore an advantage of our superresolution algorithm is its capability of improving image detail in highly noisy data such as the IR sequences with the low contrast and signal-to-noise ratio.



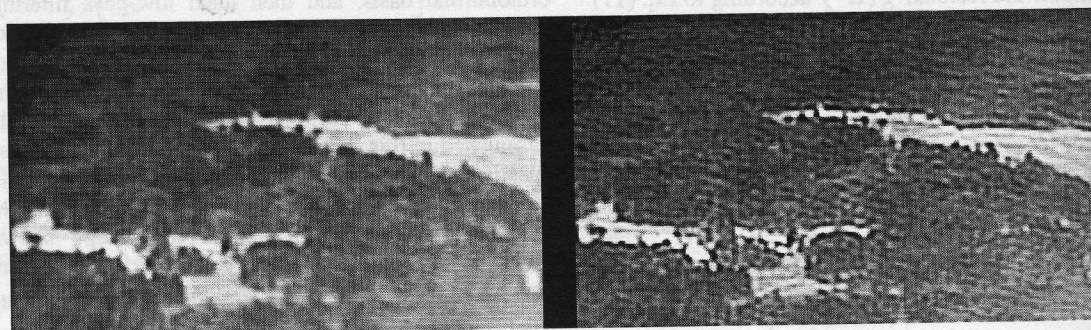
2a). 184 × 108 input frame 01 from DIM01 sequences.

2b). Bilinear interpolation of frame 01.



2c). Average of all the low-resolution images.

2d). Superresolution image by the proposed method



2e). Superresolution image by gradient descent method.

2f). Superresolution image by the IBP method

Figure 2. High-reconstruction results of IR sequences by different superresolution approaches.

For comparison with the proposed scheme, the IBP and the gradient descent methods were used in the experiment to the same image sequences. Figures 2e, 2f show the results. All the three approaches improve the spatial resolution with respect to the original IR sequence images. However, the IBP scheme leads to a poor estimate due to high noisy images. This method directly minimizes the total squared error between the entire model predicted low-resolution data and the observed low-resolution data. The effects of noise are not incorporated into the iterative process in the IBP method. The proposed scheme and the gradient descent scheme add a constraint term that attempts to improve the behavior of reconstruction algorithm by incorporating the prior information. Thus, the two methods exhibit robustness to high noisy images. In addition, the proposed approach converges fast because the estimation errors in high-frequency and low-frequency bands are processed separately. The gradient descent approach required 7 iterations prior to convergence.

## 5. Conclusions

We propose a new superresolution reconstruction algorithm to enhance the spatial resolution of IR image sequences. This approach places the multi-frame wavelet expansions into a Bayesian framework to form a MAP estimate of the desired high-resolution image. In this approach, both of the image sequences and the degradation operator to be inverted are represented by wavelet expansions. Minimizing the regularization cost function based on wavelet expansion forms the high-resolution estimate. This provides a unified approach for deblurring, noise removal, and high-resolution reconstruction from a low-resolution, blurred, and noisy infrared image sequence. Experimental results demonstrate that the proposed method is an effective algorithm to improve image detail of the IR sequences, which is highly noisy and of low contrast. Convergence speed of proposed scheme is faster than that of the IBP and gradient descent methods because the estimation errors in high-frequency and low-frequency bands are processed separately.

A number of issues will be explored in future research. High-precise alignment and the effect of the number of input images on results are the most critical aspects. In addition, image quality evaluation for the reconstructed result derived from different superresolution approaches will be discussed.

## References

- [1]. R.C. Gonzalez and P. Wintz, *Digital Image Processing*. New York: Addison-Wesley, 1987.
- [2]. A.K. Jain, *Fundamentals in Digital Image Processing*. Englewood Cliffs, NJ: Prentice-Hall, 1989.
- [3]. A.K. Katsaggelos, Iterative image restoration algorithms. *Optical Engineering*, Vol.28, No.7, pp.735-748, July 1989.
- [4]. A.K. Katsaggelos, A multiple input image restoration approach. *J. Vis. Commun. Image Representat.*, Vol.1, pp.93-103, Sept. 1990.
- [5]. B.R. Hunt and O. Kubler, Karhunen-Loeve multispectral image restoration, Part I: Theory. *IEEE trans. Acoust., Speech, Signal Processing*, Vol. ASSP-32, pp.592-599, June 1984.
- [6]. A.J. Patti, A.M. Tekalp and M. I. Sezan, Image sequence restoration and de-Interlacing by motion-compensated Kalman filtering, *SPIE*, Vol. 1903, 1993.
- [7]. T.S. Huang and R.Y. Tsay, Multiple frame image restoration and registration. *In Advanced in Computer Vision and Image Processing*, Vol.1, T.S. Huang, Ed. Greenwich, CT: JAI, pp.317-339, 1984.
- [8]. S.P.Kim, N.K. Bose, and H.M. Valenzuela, Recursive reconstruction of high-resolution image from noisy undersampled multiframe. *IEEE trans. Acoust., Speech, Signal Processing*, Vol.38, pp.1013-1027, June 1990.
- [9]. M. Irani and S. Peleg, Improving resolution by image registration. *CVGIP: Graph. Models Image Process.*, Vol.53, pp.231-239, Mar. 1991.
- [10]. R.R. Schultz and R.L. Stevenson, Improved definition video frame enhancement. *IEEE int. Conf. Acoustics, Speech, and Signal Processing (ICASSP)*, Detroit, MI, May 1995, Vol. IV, pp.2169-2172.
- [11]. M. Elad and A. Feuer, Restoration of a Single superresolution image from several blurred, noisy, and undersampled measured Images. *IEEE trans. Image Process.*, Vol.6, No.12, Dec. 1997.
- [12]. C. Srinivas and M.D. Srinath, A stochastic model-based approach for simultaneous restoration of multiple miss-registered images. *SPIE*, Vol.1360, pp.1416-1427, 1990.
- [13]. S. Cain, R.C. Hardie, and E.E. Armstrong, Restoration of aliased video sequences via a maximum-likelihood approach. *In National Infrared Information Symposium (IRIS) on Passive Sensors*, Monterey, CA (Mar. 1996).
- [14]. R.C. Hardie, K.J. Barnard, J.G. Bognar and E.A. Watson, High-resolution image reconstruction from a sequence of rotated and translated frames and its application to an infrared imaging system. *Optical Engineering*, Vol.37, No.1, pp.247-260, Jan. 1998.

- [15]. T.R. Tuinstra and R.C. Hardie, High-resolution image reconstruction from digital video by exploitation of nonglobal motion. *Optical Engineering*, Vol.38, No.5, pp.806-814, May 1999.
- [16]. F.O. Baxley and R.C. Hardie, Application of multiframe high-resolution image reconstruction to digital microscopy. *Applied Optics*, Vol.38, No.11, pp.2263-2269, April 1999.
- [17]. H. Stark and P. Oskoui, High-resolution image recovery from image-plane arrays, using convex projections. *J. Opt. Soc. Amer. A*, Vol.6, No.11, pp.1715-1726, 1989.
- [18]. A.M. Tekalp, M.K. Ozkan, and M.I. Sezan, High-resolution image reconstruction from lower-resolution image sequences and space varying image restoration. *IEEE int. Conf. Acoustics, Speech and Signal Processing (ICASSP)*, San Francisco, CA., Vol. III, pp.169-172, Mar. 1992.
- [19]. A.J. Patti, M.I. Sezan, and A.M. Tekalp, Superresolution video reconstruction with arbitrary sampling lattices and nonzero aperture time. *IEEE trans. Image Process.*, Vol.6, No.8, pp.1064-1076, Aug. 1997.
- [20]. H. Shekarforoush and R. Chellappa, Data-driven multichannel superresolution with application to video sequences. *J. Opt. Soc. Am. A*, Vol.16, No.3, pp.481-492, Mar. 1999.
- [21]. R.R. Schultz and R.L. Stevenson, Extraction of high-resolution frames from video sequences. *IEEE trans. Image Process.*, Vol.5, No.6, pp.996-1011, June 1996.
- [22]. Gaofeng Wang, Jun Zhang, and Guangwen Pan, Solution of inverse problems in image processing by Wavelet expansion. *IEEE trans. Image Processing*, Vol.4, No.5, pp.579-593, May 1995.
- [23]. S. Mallat, A theory for multiresolution signal decomposition: The wavelet representation. *IEEE trans. Pattern Anal. Machine Intell.*, Vol. PAMI-11, pp.674-693, July 1989.
- [24]. I. Daubechies, Orthonormal bases of compactly supported wavelets. *Commun. Pure Appl. Math.*, Vol.41, pp.909-996, Nov. 1988.